Contents lists available at ScienceDirect

Bioorganic & Medicinal Chemistry Letters

journal homepage: www.elsevier.com/locate/bmcl

Bioorganic & Medicinal Chemistry Letters Vol. 19, No. 8, 2009

Contents

ARTICLES

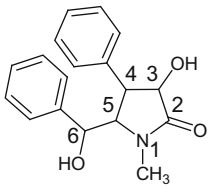

1 (3S,4R,5R,6S) **2** (3R,4S,5S,6R)
3 (3R,4S,5R,6S) **4** (3S,4R,5S,6R)
5 (3R,4S,5R,6R) **6** (3S,4R,5S,6S)
7 (3R,4R,5R,6S) **8** (3S,4S,5S,6R)
9 (3R,4R,5S,6R) **10** (3S,4S,5R,6S)
11 (3R,4R,5S,6S) **12** (3S,4S,5R,6R)
13 (3R,4R,5R,6R) **14** (3S,4S,5S,6S)
15 (3S,4R,5R,6R) **16** (3R,4S,5S,6S)

The synthesis and activity in enhancing LTP of 16 (8 pairs) optically pure stereoisomers of clausenamide with four chiral centers are reported.

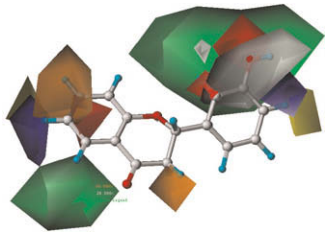

To identify the structural requirements that are pivotal in enhancing Early growth response-1 (Egr-1) expression, the quantitative relationships between the structural properties of flavanone derivatives and their increments of Egr-1 expression were elucidated.

5-Alkyl and aryl-pyrazole–tetrazoles have been identified as a new class of selective, small-molecule, agonists of the human G-protein-coupled receptor GPR109a, a high affinity receptor for the HDL-raising drug nicotinic acid.

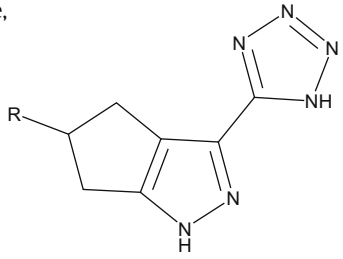

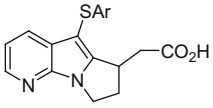

Potent and selective azaindole DP1 receptor antagonists were identified.

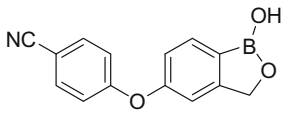

5b (AN2728)

Anti-inflammatory activity and SAR of novel benzoxaborole derivatives are reported.

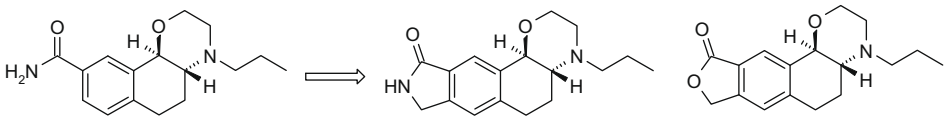

(R,R)-**2**

pKi D_3 = 7.7
Ki D_2/KiD_3 = 40

(R,R)-**15**

pKi D_3 = 8.4
Ki D_2/KiD_3 = 199

(R,R)-**16**

pKi D_3 = 8.1
Ki D_2/KiD_3 = 250

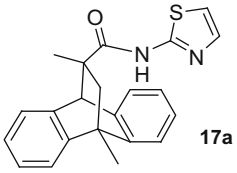

17a

A series of dihydro-9,10-ethano-anthracene-11-carboxamides as novel glucocorticoid receptor modulators is reported. SAR exploration identified compounds from this series displaying a promising dissociation profile in discriminating between transrepression and transactivation activities. **17a** is a partial agonist of GR-mediated transactivation which elicits potent and efficacious transrepression in reporter gene assays. A hypothetical binding mode is provided which accounts for the induction of functional activity by a bridgehead methyl group.

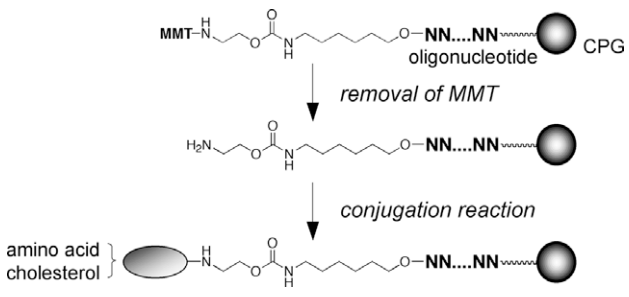

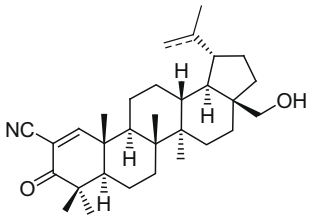

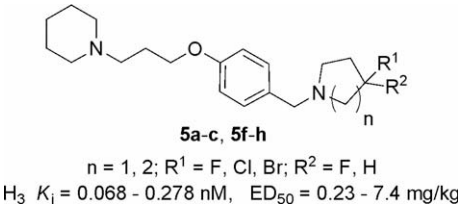

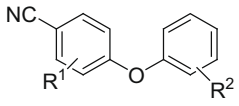

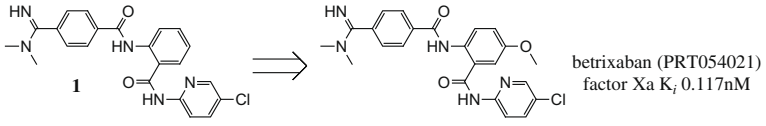

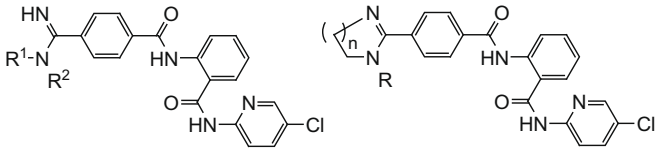

An anthranilamide-based benzamidine and its N-substituted analogs were designed and examined as factor Xa inhibitors, using the N-substituted benzamidines as unconventional S4 binding element. A group of *N,N*-dialkylbenzamidines have been discovered as potent factor Xa inhibitors with strong anticoagulant activity and promising oral PK profiles.

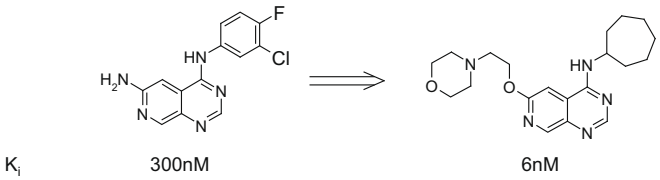

SAR and CNS penetration of a series of novel mgluR1 antagonists is described. The multiple of the unbound K_i in cerebrospinal fluid necessary to give morphine like analgesic effects in an electromyograph pinch model in rodents is given.

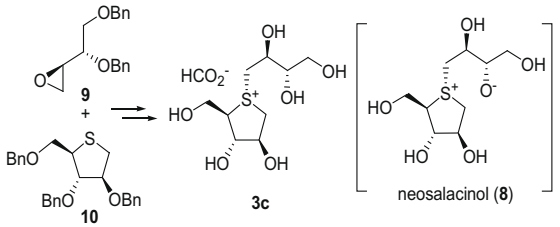

The structure of neosalacinol (**8**), a potent α-glucosidase inhibitor isolated recently from Ayurvedic medicine *Salacia oblonga*, was revised to salacinol de-*O*-sulfate (**3c**), by comparison of the spectroscopic properties of **8** with an authentic specimen synthesized by the coupling reaction of **9** and **10**.

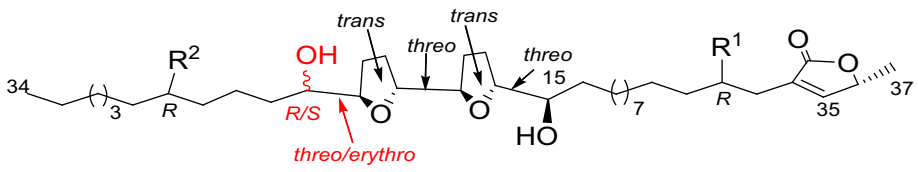

Twelve annonaceous acetogenins (ACGs) with different stereochemical structures and configuration were selected to test for their inhibitions on the growth of Hela, SMMC-7541, SGC-7901, MCF-7 and A-5408 tumor cell lines using MTT method. This was the first to simultaneously investigate effects of structural factors of stereochemical structures and configuration on cytotoxicities with structure–activity relationship.

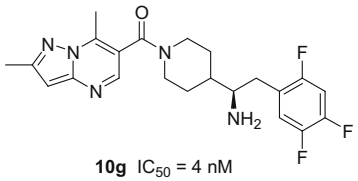

10g IC_{50} = 4 nM

Utilizing parallel synthesis and a high-throughput in vitro micronucleus assay enabled the identification of **10g**, a highly DPP-IV selective compound with an acceptable human DPP-IV inhibition profile based on the rat PK/PD model and a projected human dose that was suitable for clinical development.

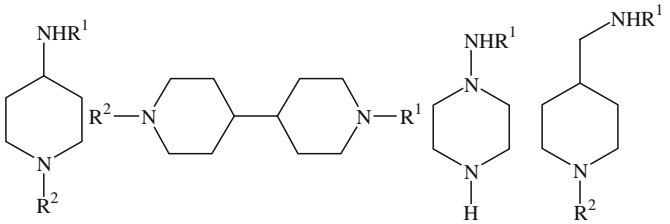

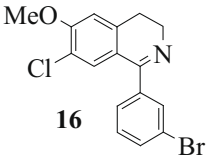

16

A series of 1-aryl-3,4-dihydroisoquinoline inhibitors of JNK3 are described. Compounds **20** and **24** are the most potent inhibitors (pIC50 7.3 and 6.9, respectively in a radiometric filter binding assay), with 10- and 1000-fold selectivity over JNK2 and JNK1, respectively, and selectivity within the wider mitogen-activated protein kinase (MAPK) family against p38α and ERK2. X-ray crystallography of **16** reveals a highly unusual binding mode where an H-bond acceptor interaction with the hinge region is made by a chlorine substituent.

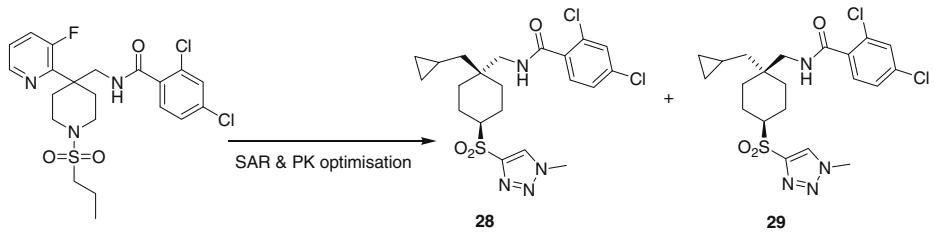

28 **29**

A series of heterocyclic sulfonamides have been developed which are potent and selective inhibitors of hGlyT1. SAR studies to optimise the in vitro and in vivo properties are described. Optimisation of the central scaffold resulted in cyclohexane sulfones **28** and **29**, which have good PK properties and show promise for further development.

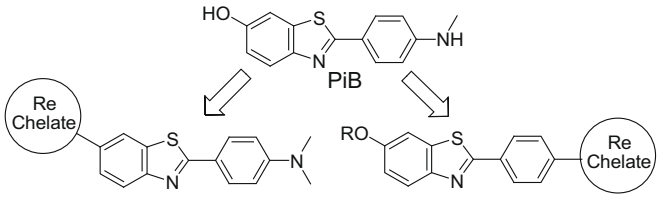

K_i= 10.0 - 88.6 nM

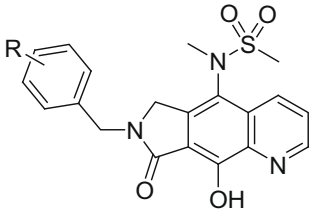

R	3-Cl-4-F	5-Cl-2,4-F
IC_{50}	52 nM	39 nM
EC_{50}(10%FBS)	3.5 nM	6 nM
EC_{50}(HSP)	12 nM	17 nM
$t_{½}$ (rat iv)	1.36 hr	1.38 hr
(dog iv)	7.13 hr	16 hr

SAR studies on the *para*-fluorobenzyl moiety of tricyclic HIV integrase inhibitors are discussed and lead compounds with potency and PK properties comparable to raltegravir were identified.

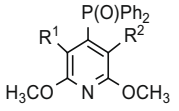

R^1 = H/Br R^2 = H/Br/Ph

The preparation of 2,6-disubstituted pyridinyl phosphine oxides and their antitumor properties were reported.

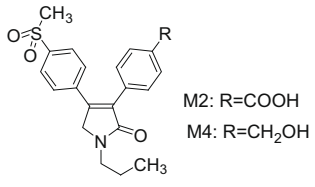

The synthesis and anti-inflammatory activity of two moderately selective COX-2 inhibitors M2 and M4, as the major metabolites of imrecoxib, is reported.

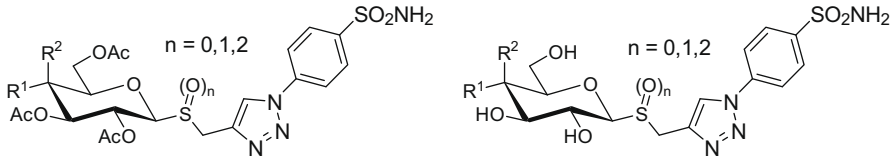

Glucose: R^1 = OAc (or OH), R^2 = H
Galactose: R^1 = H, R^2 = OAc (or OH)

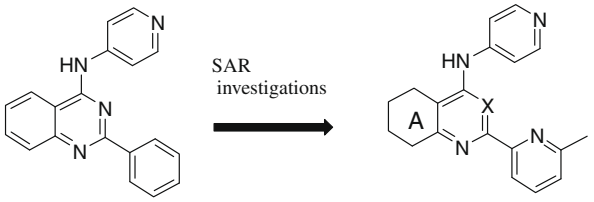

3a A=phenyl, X=N, **3d**

Starting from quinazoline **3a**, we identified **3d** a potent and selective ALK5 inhibitor over p38MAP kinase suitable for oral administration.

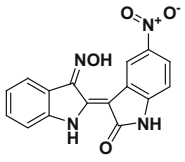

Based on the β-catenin-drived Wnt activator of 6-bromoindirubin-3′-oxime (BIO), indirubin analogs were evaluated for β-catenin-mediated gene expression. A novel indirubin analog, indirubin-5-nitro-3′-oxime (INO), was considered a potential activator, and structure–activity studies were conducted with indirubins.

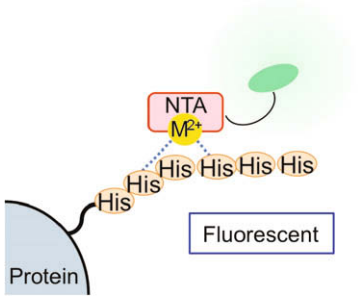

A novel fluorescein-based probe is reported. This molecule shows selective fluorescence enhancement on binding to a hexahistidine tag on the protein surface.

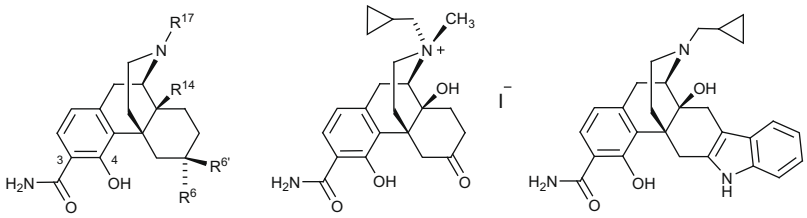

High binding affinity [K_i values (μ) = 0.072–1.3 nM] to opioid receptors is seen in a novel series of 3-desoxy-3-carboxamido-4-hydroxymorphinans where the carboxamide group is stabilized in the putative bioactive conformation.

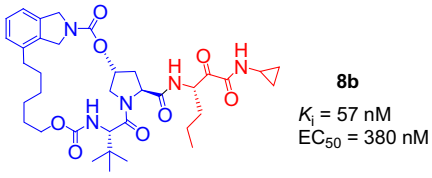

Design, synthesis and biological evaluation of a new series of hepatitis C virus (HCV) NS3/4A protease inhibitors bearing a P2-P4 macrocycle and a P1-P1′ α-ketoamide warhead is described.

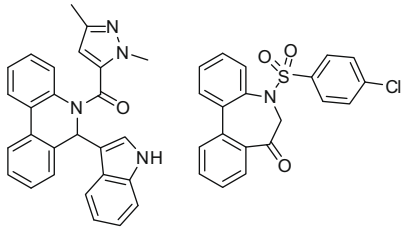

Applying vHTS based on a homology model, potent inhibitors of K_V1.3 and IK-1 were identified.

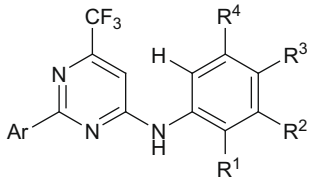

The synthesis and SAR studies of the 2-aryl group of 4-anilino-2-arylpyrimidines as novel apoptosis inducers are reported.

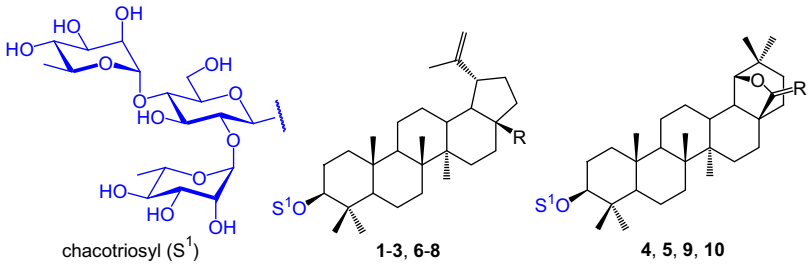

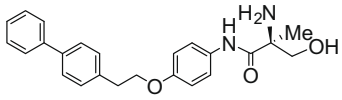

11c (PPI-4667)

In pursuit of potent and selective sphingosine-1-phosphate receptor agonists, further SAR expansion on our previously reported scaffolds led to discovery of novel series of molecules with excellent in vitro and in vivo potency in both mouse and rat models.

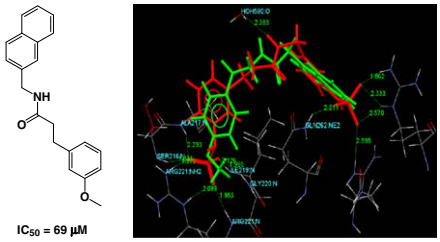

Structure of the most potent compound (**3a**) and its binding pose (in red colour) into the active site gorge of PTP-1B enzyme as compared to the X-ray crystal based binding pose of the control (PDB-ID: 2F70)

Structure of the most potent compound (**3a**) and its binding pose (in red colour) into the active site gorge of PTP-1B enzyme as compared to the X-ray crystal based binding pose of the control (PDB-ID: 2F70).

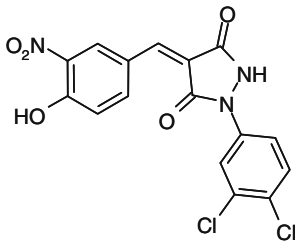

The QSAR analysis of 34 pyrazolidine-3,5-diones derivatives of HCD160 showed that the presence of the 3-nitro-4-hydroxyphenyl moiety enhanced the inhibition activity for Dyrk1A.

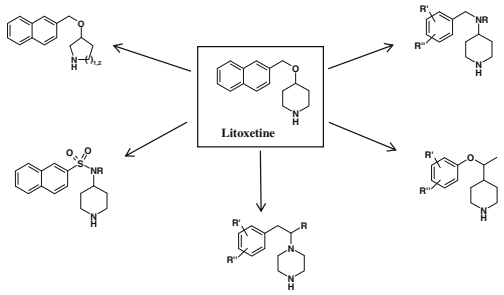

The reported selective serotonin Re-uptake Inhibitor (SSRI) litoxetine was used as the starting point in the design of a range of potent, selective SSRIs with high ease of synthetic accessibility.

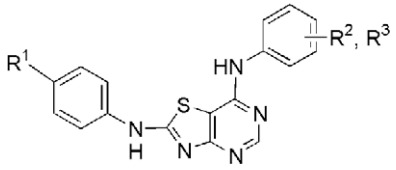

2,7-Diamino-thiazolo[4,5-*d*]pyrimidines analogues were synthesized as novel epidermal growth factor receptor (EGFR) tyrosine kinase inhibitors. Representative compounds showed potent and selective EGFR inhibitory activities and inhibited in vitro cellular proliferation in EGFR-overexpressing human tumor cells. The synthesis and preliminary biological, physical, and pharmacokinetical evaluation of these thiazolopyrimidine compounds are reported.

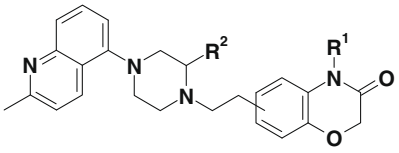

8-[2-(4-Aryl-1-piperazinyl)ethyl]-2*H*-1,4-benzoxazin-3(4*H*)-ones have been identified as highly potent 5-HT$_{1A/B/D}$ receptor antagonists with and without additional SerT activity and a high degree of selectivity over hERG potassium channels. Modulation of the different target activities gave compounds with a range of profiles suitable for further in vivo characterization.

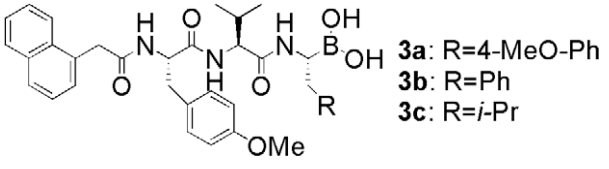

Synthesis of boronic acid derivatives (**3a**–**c**) of tyropeptin, proteasome inhibitors, are reported.

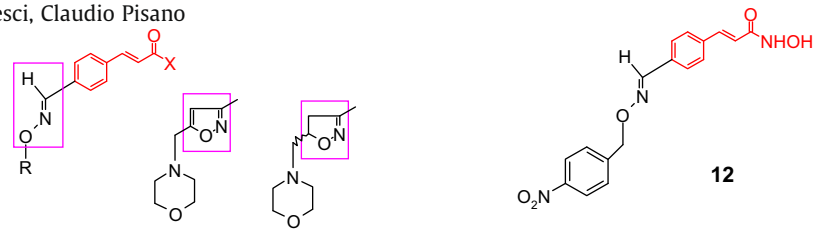

A small library of N-based scaffold derivatives has been described. SAR has been established for R, oxyme moiety and X cinnamoyl-based HDAC inhibitors. Several 4-oxime derivatives demonstrated a promising inhibitory activity on HDAC6 and HDAC8 coupled to a good selectivity profile. Analogue **12** (ST2987) constitutes a promising lead compound for further optimization towards the identification of a clinical candidate.

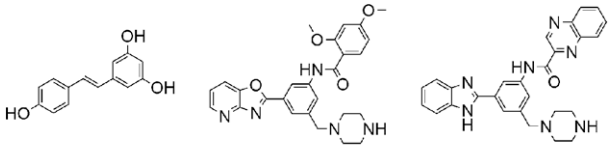

The identification and SAR of novel small molecule activators of SIRT1, which are structurally distinct and more potent than resveratrol (**1**), are described.

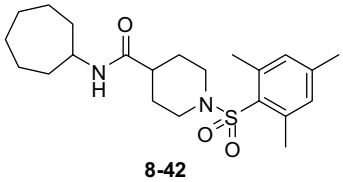

A class of potent non-urea inhibitors of soluble epoxide hydrolase was discovered via high throughput screening and SARs-guided modification.

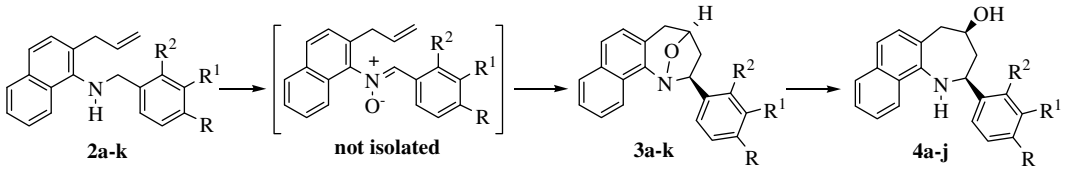

OTHER CONTENTS

*Corresponding author

ⓘ+ Supplementary data available via ScienceDirect

COVER

Overlay of high resolution co-crystal structures of *R*-**22**-ADP (cyan) and **1**-ADP (green) bound in an allosteric binding site of the mitotic kinesin KSP. [Roecker, A. J.; Coleman, P. J.; Mercer, S. P.; Schreier, J. D.; Buser, C. A.; Walsh, E. S.; Hamilton, K.; Lobell, R. B.; Tao, W.; Diehl, R. E.; South, V. J.; Davide, J. P.; Kohl, N. E.; Yan, Y.; Kuo, L. C.; Li, C.; Fernandez-Metzler, C.; Mahan, E. A.; Prueksaritanont, T.; Hartman, G. D. *Bioorg. Med. Chem. Lett.* **2007**, *17*, 5677.]

Indexed/Abstracted in: Beilstein, Biochemistry & Biophysics Citation Index, CANCERLIT, Chemical Abstracts, Chemistry Citation Index, Current Awareness in Biological Sciences/BIOBASE, Current Contents: Life Sciences, EMBASE/Excerpta Medica, MEDLINE, PASCAL, Research Alert, Science Citation Index, SciSearch, TOXFILE

ELSEVIER

ISSN 0960-894X